JOURNAL OF PROPULSION AND POWER
Vol. 16, No. 5, September–October 2000

Injection and Mixing Processes in High-Pressure Liquid Oxygen/Gaseous Hydrogen Rocket Combustors

W. Mayer,* A. Schik,† and M. Schäffler‡
DLR, German Aerospace Research Center, Lampoldshausen, 74239 Hardthausen, Germany
and
H. Tamura§
National Aerospace Laboratory, Kakuda, Miyagi 981-1525, Japan

The injection, mixing, and combustion processes in a liquid oxygen (LOX)/gaseous hydrogen (GH_2) rocket engine combustor at high chamber pressures (10 MPa) are studied and modeled. An experimental LOX/GH_2 rocket motor consisting of a single coaxial shear injector element and a cylindrical chamber with optical access has been used for flow visualizations and measurements. Cold-flow injection tests utilizing liquid nitrogen and gaseous helium at elevated pressures have been done for flowfield characterization by different diagnostic methods such as flash-light photography and high-speed cinematography using a shadowgraph setup. The injection visualizations and studies under cold-flow and combusting conditions revealed a remarkable difference between subcritical spray formation and evaporation and the supercritical injection and mixing process. The study shows that approaching supercritical chamber pressures injection can no longer be regarded as a spray formation but rather as a fluid/fluid mixing process. As the flow visualizations indicate, the effect of the coaxial atomizer gas is less effective as previously expected. The flame is attached to the LOX post and develops in the LOX post wake. The observed flame holding mechanism is discussed. An evaluation of the radiation spectrum of the flame inside the combustion chamber revealed that radiation in the visible range is mainly due to water vapor.

Introduction

THE research during the last few years on liquid oxygen (LOX)/gaseous hydrogen (GH_2) injection, mixing, and combustion has led to a more profound understanding of the processes in a cryogenic rocket engine combustion chamber (Refs. 1–4 for example). Some basic phenomena of propellant injection, mixing, and combustion are well understood, though the knowledge is still not satisfactory in view of quantitative assessment of part processes, for example, turbulent mixing of reacting fluids.

Cold-Flow Injection and Mixing

To study the mixing process in cold-flow injection tests under representative conditions (real-gas effects at supercritical pressures and high Weber and Reynolds numbers) oxygen (LOX) and hydrogen H_2 were simulated by liquid nitrogen LN_2, and hydrogen H_2 or helium He, respectively.

Experimental Setup

In a cryogenic test facility (Fig. 1) the simulation fluids were injected through model injectors into a pressurized tank that simulated the combustion chamber pressure. The pressure was regulated independently from the injected mass flow rates up to 6.0 MPa. LN_2 was fed with a temperature down to 90 K, whereas He and H_2 were fed with temperatures between 100 and 370 K. The temperatures of the injected fluids were measured close to the injector exit using thermocouples (see Fig. 2). The feed lines were isolated to be able to operate with different fluid temperatures for the central jet and coaxial fluid, respectively.

Different injection conditions were studied utilizing various diagnostics. Flash-light photography and high-speed cinematography using a shadowgraph setup were used for phenomenological studies of the mixing process and for quantitative measurements of timescales and length scales at the interface between the two fluids.

Flash photography was used for phenomenological studies of the mixing process and for classifying the macroscopic jet appearance with nondimensional numbers, for example, Weber and Reynolds numbers. The shadowgraphy setup used, utilizing a 30-ns Nano-lite flash lamp (High Speed Photo Systeme) is shown in Fig. 3. The change in phenomenology with rising back pressure for the one-component-system nitrogen ($p_{crit} = 3.4$ MPa) is shown in Fig. 4. Cryogenic nitrogen (105 K) was injected with a velocity of 1 m/s into warm nitrogen (300 K) at chamber pressures of 2.0, 3.0, and 4.0 MPa. The inner injector diameter was 1.9 mm for all test cases.

Experimental Results

At the subcritical pressure of 2.0 MPa, the surface of the jet is smooth and large-scale disturbances can be seen. At 3.0 MPa, 0.4 MPa below the critical pressure, the jet looks quite different. Because of the reduced surface tension and increased aerodynamic forces, small droplets leave the jet. At the supercritical pressure of 4.0 MPa, the surface becomes a streaky interface. The cross section of the LN_2 jet is increasing downstream, like a gaseous jet. The state of the injected nitrogen changes from a liquid to a dense fluid with rising pressure. Larger structures are observed at the jet surface. The higher the environment pressure is, the wider the spray angle is. Figure 5 shows the injection of cryogenic (100 K) nitrogen with coaxially flowing warm (275 K) helium into warm (300 K) nitrogen at the same back pressures as in Fig. 4. The critical mixing temperature of the binary system nitrogen/helium is approximately 126 K. At supercritical pressure and in the range between the critical temperature of the LN_2 and the critical mixing temperature of the binary system LN_2/He, we have transcritical injection conditions. In Fig. 5, the forming of ligaments and detachment of droplets can be seen at 2.0 and 3.0 MPa, whereas at 4.0 MPa no ligament and droplet formation can be observed. The mixing between a dense and a light fluid in a turbulent shear layer takes place. At higher Reynolds numbers, the structure of the interface at supercritical and

Presented as Paper 96-2620 at the AIAA/ASME/SAE/ASEE 32nd Joint Propulsion Conference, 1–3 July 1996, Lake Buena Vista, FL, received 26 February 1998; revision received 13 September 1999; accepted for publication 6 October 1999.

*Head, Propellant and Injection Research, Space Propulsion; wolfgang.mayer@dlr.de. Member AIAA.
†Aerospace Engineer, Space Propulsion.
‡Student Aerospace Engineering, Space Propulsion.
§Head, Rocket Combustor Laboratory. Member AIAA.

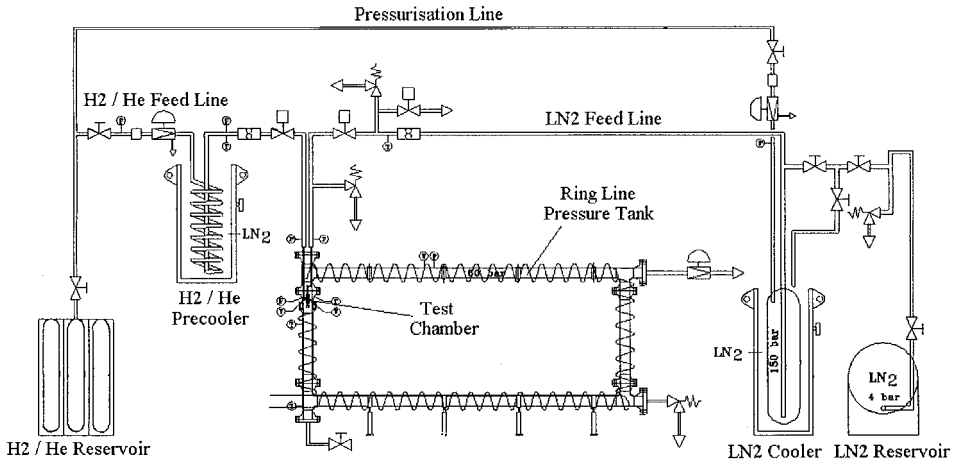

Fig. 1 Cryogenic high-pressure test facility.

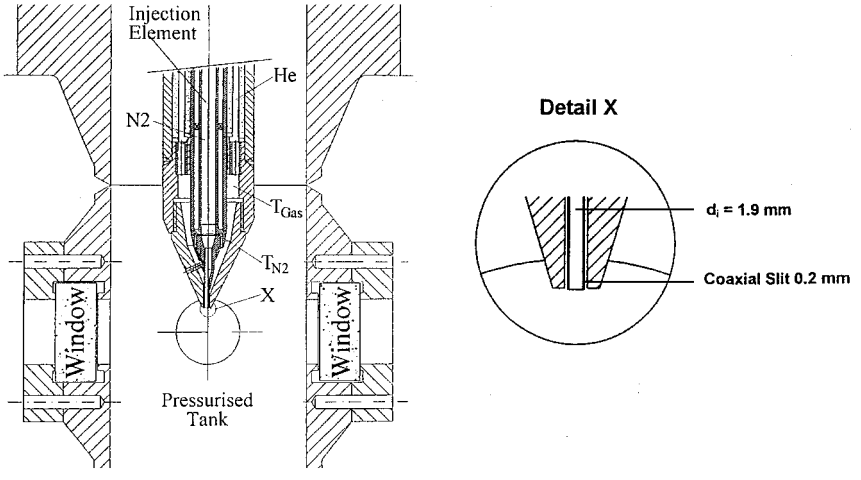

Fig. 2 Test chamber with injector and location of thermocouples.

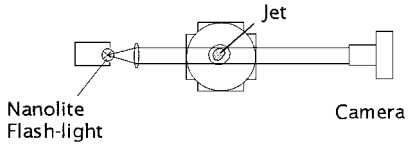

Fig. 3 Shadowgraph setup.

high subcritical pressures is similar due to the predominate influence of turbulence at reduced surface tension (see Fig. 6).

As the momentum of the coaxial gas increases with increasing chamber pressure at constant injection velocity, the aerodynamic effect leads to more and more smaller structures detached from the central jet. This tendency is well documented and proofed by the theoretical jet stabiliy analysis and experiments (for example, see Refs. 2 and 5). However, when approaching and exceeding the critical point, the surface tension decreases. The vanishing capillary forces cause a change in the atomization mechanism with larger structures at the jet surface as observed in this study.

Another important finding is that the LN_2 structures are (except very close to the injector) bent backward in the opposite direction of the coaxial atomizer gas. This indicates that the relative velocity between the central jet and the annular jet rapidly disappears. The atomization and mixing are only weakly influenced by the momentum of the coaxial gas.

LOX/GH2 Hot-Fire Tests

To study injection under combusting conditions, an experimental rocket motor with optical access has been used, and injection and mixing have been studied under cold-flow and firing conditions using flow visualization techniques.[3]

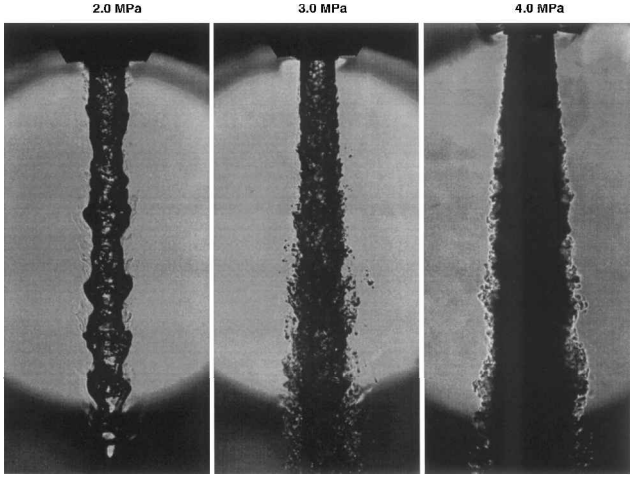

Fig. 4 LN_2 injection into GN_2: d_{LN_2} = 1.9 mm, v_{LN_2} = 1 m/s, T_{LN_2} = 105 K, left: p_{ch} = 2.0 MPa, center: p_{ch} = 3.0 MPa, and right: p_{ch} = 4.0 MPa.

Experimental Setup

An experimental rocket motor with two flat windows in opposite walls has been developed. It consists of an injector head with a single shear coaxial element; a circular, uncooled combustion chamber, with a length and a diameter of 400 and 40 mm, respectively; and a variable (exchangeable) nozzle.

The window section was cooled by a layer of GH_2. The purge flow was injected parallel to the windows in the direction of the

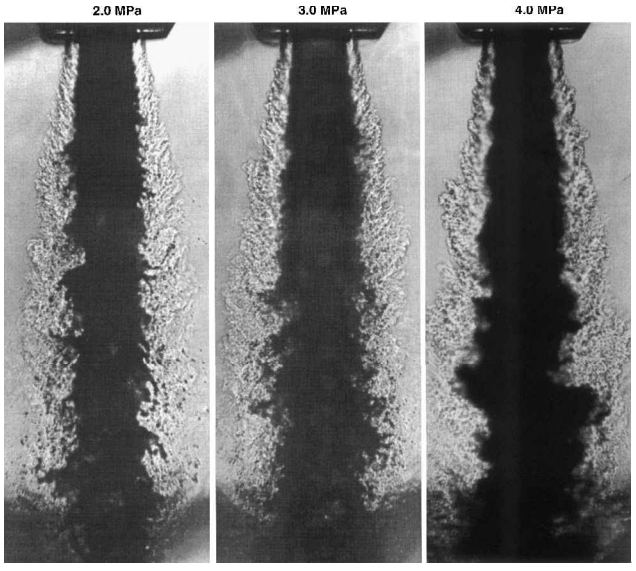

Fig. 5 LN_2 injection with coaxial gaseous helium (GHe) in a GN_2 environment; variation of chamber pressure at constant jet velocities d_{LN_2} = 1.9 mm, y_{GHe} = 0.2 mm, v_{LN_2} = 5 m/s, T_{LN_2} = 100 K, V_{He} = 50 m/s, T_{He} = 275 K; left: p_{ch} = 2.0 MPa, center: p_{ch} = 3.0 MPa, and right: p_{ch} = 4.0 MPa.

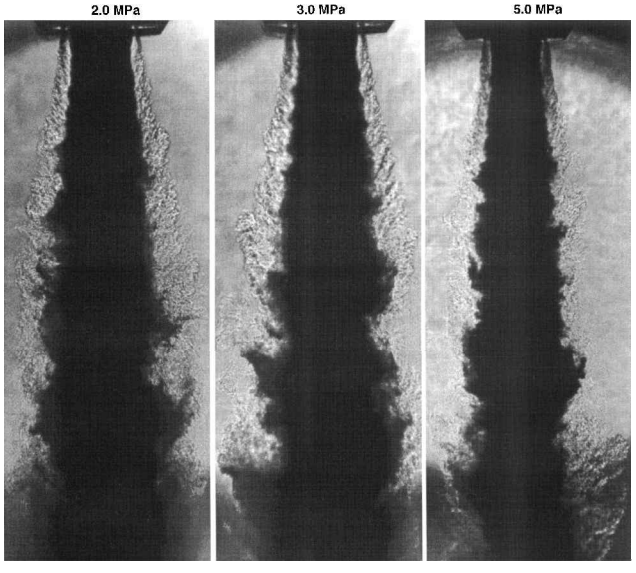

Fig. 6 LN_2 injection with coaxial GHe in a GN_2 environment; variation of chamber pressure at constant jet velocities d_{LN_2} = 1.9 mm, y_{GHe} = 0.2 mm, v_{LN_2} = 20 m/s, T_{LN_2} = 90 K, V_{He} = 200 m/s, T_{He} = 275 K; left: p_{ch} = 2.0 MPa, center: p_{ch} = 3.0 MPa, and right: p_{ch} = 4.0 MPa.

nozzle. Metal dummy windows with thermocouples were used to develop the startup and shutdown sequence and a suitable window cooling technique.

LOX was supplied to the test section from a helium-pressurized, vacuum-jacketed, 90-m^3 storage tank (see Fig. 7). The supply of GH_2 to the injector and window purge ports was from a 20.0-MPa bottle depot. To cool the cryogenic supply line, a liquid nitrogen cooling jacket was installed onto this line between the LOX tank and LOX dome. Chilling down of the LOX line made it possible to reach steady-state firing conditions in less than 1 s. Ignition was done by a small gaseous oxygen/hydrogen pilot flame. The igniter was mounted on the lower part of the chamber wall. Typical duration of a firing was 5 s, including startup transients of approximately 0.1 s. A nontapered shear coaxial injector without recess was evaluated. The injector baseline dimensions were an outer diameter d_a of 3.9 mm and a LOX post inner diameter d_i of 1 mm with a LOX post tip wall thickness of 0.3 mm (Fig. 8).

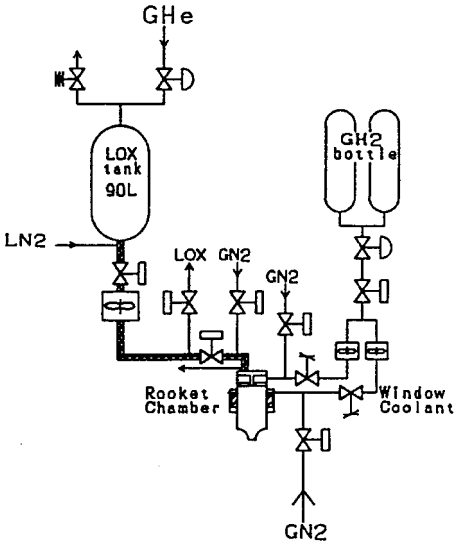

Fig. 7 Schematic of LOX/GH2 test facility.[3]

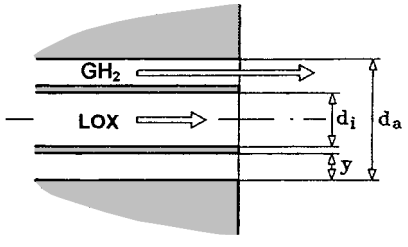

Fig. 8 Coaxial injector.

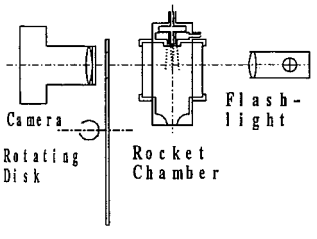

Fig. 9 Shadowgraph setup for hot-fire tests.[3]

More details of the technical setup and the results of the visualization studies were presented by Mayer and Tamura.[3] The injection visualizations and studies under combusting conditions revealed a remarkable difference between the subcritical spray formation and evaporation and the supercritical injection and mixing processes. The study shows that approaching supercritical chamber pressures, injection can no longer be regarded as an atomization or spray formation process. Under these conditions droplets no longer exist. The visualizations revealed that, at chamber pressures equal to or higher than 4.5 MPa, oxygen forms threadlike or stringylike structures that rapidly dissolve. This coincides with the results of the LN_2/He cold-flow tests under supercritical pressure conditions (see the preceding section).

Flame Holding Mechanism

In this study LOX post tip thickness was 0.3 mm and the LOX and GH_2 velocities were varied in the range from 10 to 30 m/s and 200 to 300 m/s, respectively. The propellant temperatures were 100 K for the LOX and varied between 150 and 300 K for the hydrogen. The effect of chamber pressure on the flame holding mechanism was investigated in the range from 1.0 to 10.0 MPa. For a schematic of the optical setup, see Fig. 9.

The experimental study of Mayer and Tamura[3] demonstrated that for all of these steady-state combusting conditions the flame was attached to the LOX post tip. The flame always develops between the propellants in the wake of the LOX post (see Fig. 10). Figure 10 shows two photographs of the burning coaxial jet taken by two

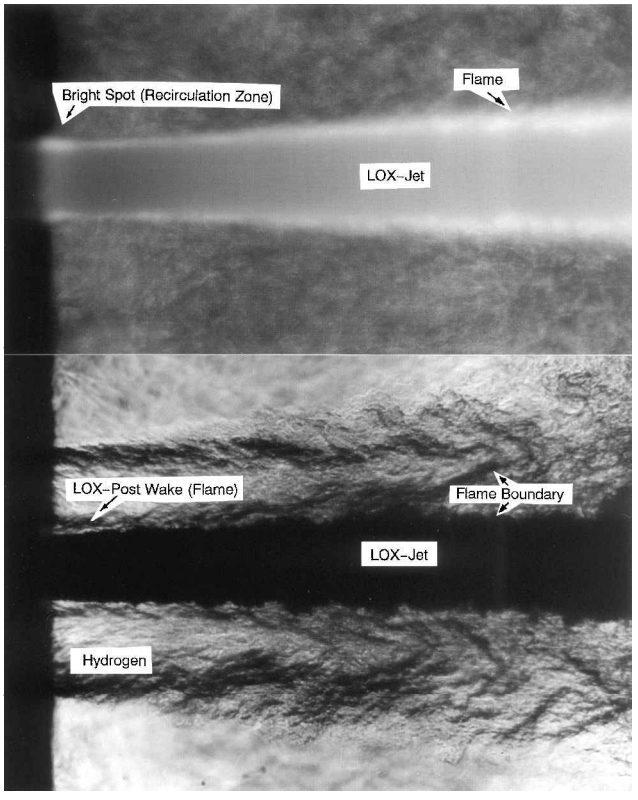

Fig. 10 Visualization of near injector region, combusting condition: flame (top) and corresponding flowfield (bottom), oxygen and hydrogen velocities are 30 and 300 m/s, respectively, d = 1 mm, and chamber pressure is 4.5 MPa (Mayer and Tamura[3]).

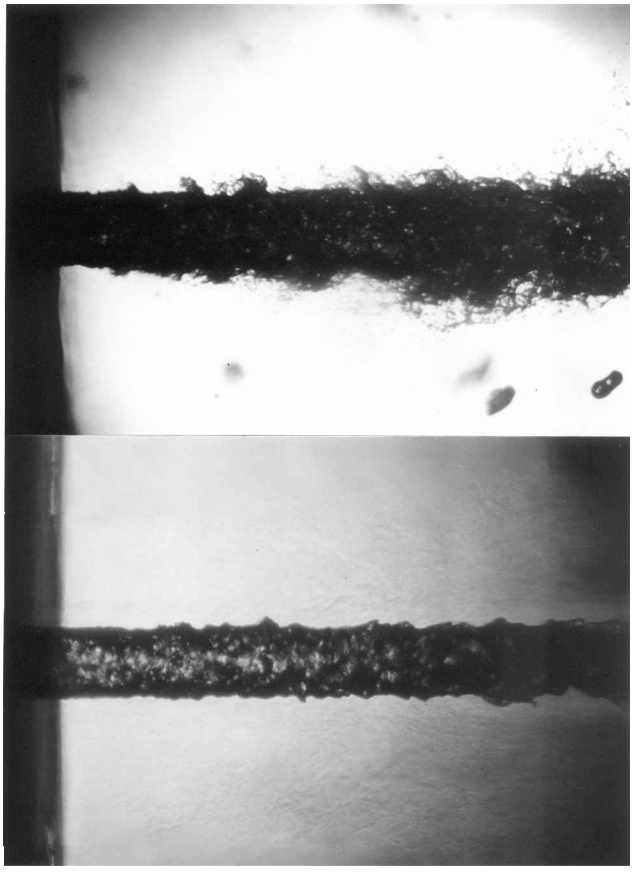

Fig. 11 LOX jet, near injector region, LOX velocity 10 m/s, hydrogen velocity 300 m/s, chamber pressure 1.5 MPa, d = 1 mm; left: burning condition and right: cold-flow injection before ignition.[3]

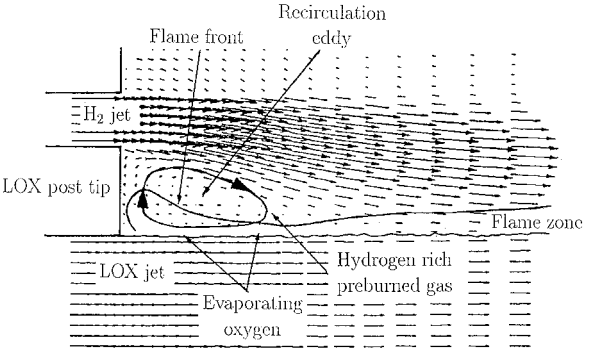

Fig. 12 Principal schematic of flame-holding mechanism.

different visualization techniques under the same firing conditions. The upper photograph shows the flame vizualization using a standard photography setup; the bottom photograph shows the corresponding flowfield visualization utilizing a shadowgraph setup.

Figure 11 demonstrates the effect of the flame on the LOX jet as a comparison of cold-flow injection and injection under firing condition. In both cases, the chamber pressure is 1.5 MPa. LOX and GH_2 are injected at temperatures of 100 K. The top of Fig. 11 shows the cold-flow atomization of LOX/GH_2 in an oxygen/hydrogen environment. In the cold-flow case, fine oxidizer threads and droplets are visible. No density gradient is visible between the GH2 and ambient gases. After ignition, in the combusting case the fine surface structures rapidly vaporize, and droplets are never formed in the near injector region. No detached LOX ligaments or droplets can be observed in the vicinity of the injector. The remarkable smoothness of the LOX jet under combusting conditions is in part due to the rapid vaporization of the oxygen surface waves. On the other hand, the density of the hot reaction zone (3500 K) is very low, especially at low chamber pressures, causing a considerable reduction of aerodynamic interaction between the LOX jet and the hydrogen. At higher chamber pressures (4.0 MPa and higher) the LOX jet looks somewhat more wavy, but no ligament detachment could be observed.

We can conclude that if heating rates are high diffusion processes can predominate prior to atomization.

It seems that we have a flame stabilization mechanism that is based on the back flow of hydrogen and precombusted gases driven by several small recirculation eddies in the vicinity of the LOX-post tip (see Fig. 12). There, the flow velocities are partly low enough that stationary combustion is possible. Near the LOX jet, the flow runs in the direction toward the face plate (upstream in view of the main flow direction). The downstream part of the recirculation eddy consists of partly preburned, but hydrogen rich, combustion gases. Near the LOX jet surface, the evaporating oxygen mixes into this gas and combusts. The combusted gas again mixes into the hydrogen jet and partly recirculates back.

Therefore, the flame-holding mechanism is based on the principle of a diffusion flame. We can assume that the energy for the LOX evaporation mainly comes from the hot recirculating combustion gases. However, it is still not evident if the energy transport is solely due to convective heat transfer, or radiation of flame additionally plays a role.

Radiation of Flame

It resulted that the flame of LOX/hydrogen combustion radiates in a continous range between infrared (IR) and UV. The dependency of line intensities on mixture ratio O/F was small indicating that the combustion gases were undergoing various degrees of reaction with a wide distribution in gas temperature and composition. The measurements demonstrated that between 1.0- and 10.0-MPa chamber pressure the flame spectrum (wavelength band) is similar, but the radiation intensity R increases dramatically with pressure ($R \propto p_{ch}^{2.0,\ldots,3.2}$). Another important observation was that radiation intensity increases with downstream distance. Detailed radiation measurements can be found by Mayer and Tamura.[3] Figure 13 shows the radiation spectrum in the range between 290 and 360 nm at

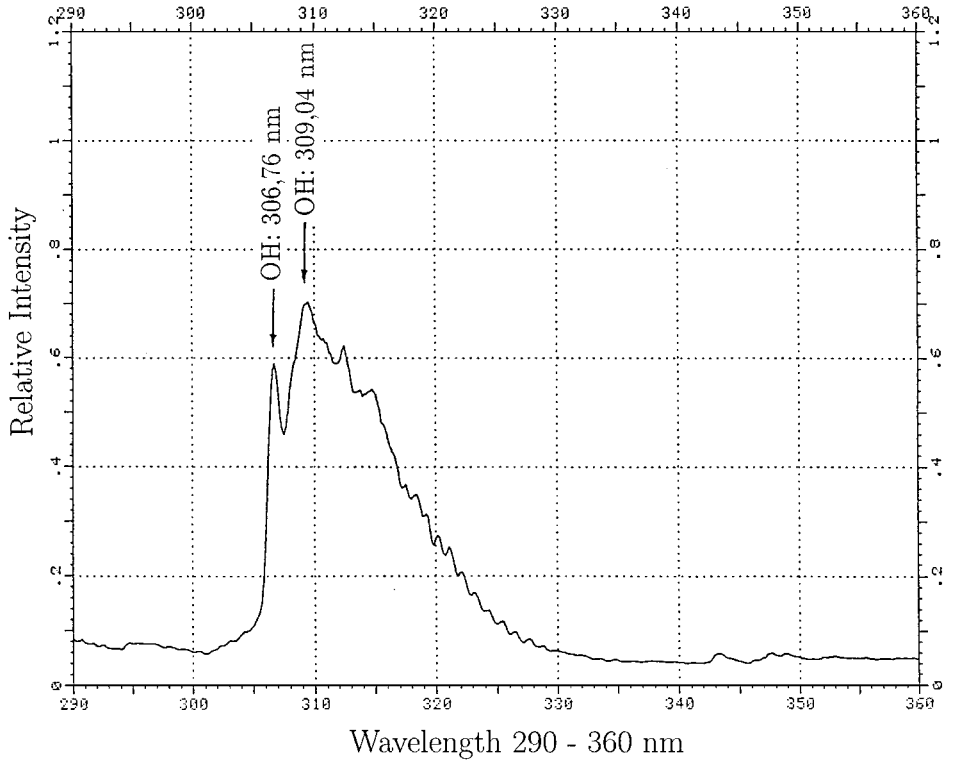

Fig. 13 Spectra of LOX/hydrogen flame, range 290–360 nm and p_{ch} = 6.0 MPa, measured 70 mm downstream from face plate.

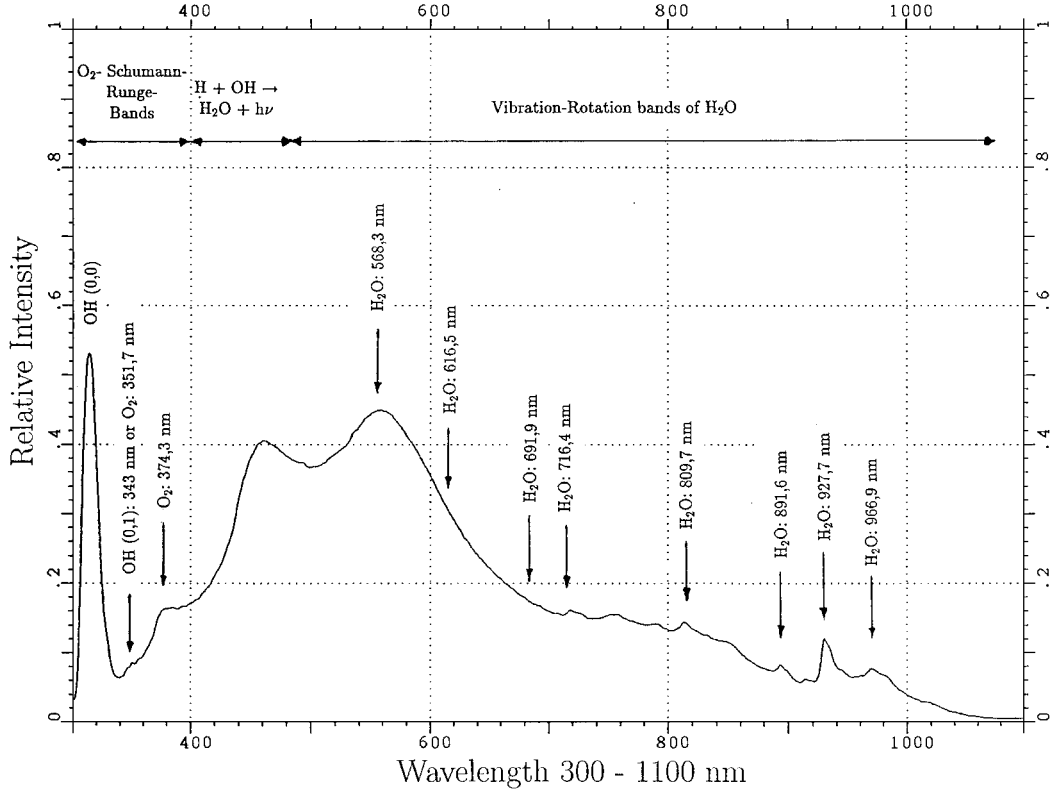

Fig. 14 Spectra of LOX/hydrogen flame, range 300–1100 nm and p_{ch} = 6.0 MPa, measured 70 mm downstream from face plate.

6.0 MPa chamber pressure with spectrometer resolution of 0.9 nm. The OH peaks around 306.76 and 309.04 nm can be identified. A preliminary evaluation of the spectrum in the range 300–1100 nm, with a spectral resolution of 1.7 nm again at 6.0-MPa chamber pressure is shown in Fig. 14. The OH peak is easily identified in the UV range. A number of peaks could be assigned to H_2O bands, whereas some seem to come from O_2 emissions.

The peak identification has been done in reference to the flame spectra measurements published by Gaydon.[6]

Diagnostics

To understand and model combuster processes, quantitative measurements of species, density, temperature, and velocity distribution are essential. Flow visualization techniques such as flash-light photography and high-speed cinematography proved to be powerful tools for phenomenological studies. Laseroptical diagnostic means such as Coherent Anti-Stokes Raman Spectroscopy or linear Raman scattering have, on principle, potential for quantitative measurements of reacting gas flows at low pressures (for example,

see Foust et al.[7]). However, the strong radiation of the flame in the whole range between IR and UV seems to limit the applicability of such methods for high-pressure LOX/GH_2 combustors. The density gradients, that is, gradients of the refraction index in such a flow, further the problem: The location of the source and signal origin is no longer possible. Alternative diagnostics have to be investigated.

Despite some difficulties in technical realization, diagnostics in the x-ray range looks somewhat promising.[8] Neither density gradients nor radiation influence the result of x-ray diagnostics. For example, in a shadowgraph setup with an x-ray flash lamp, one receives a quantitative accessible picture of the density distribution in the combustion chamber. Preliminary promising results utilizing an x-ray flash-lamp setup of a water jet in a coaxial air stream have been received. A further qualification of this method is essential.

Conclusions

Cold-flow injection experiments have highlighted the effect of pressure on the atomization and mixing of cryogenic propellants.

The tendency of smaller drops and ligaments at increased aerodynamic pressure of the coaxial gas changes as the effect of capillary forces decreases in the transcritical region. Because of the vanishing capillary forces in the trans- and supercritical region, a change of the atomization mechanism and tendencies could be observed.

The flow visualizations indicate that the relative velocity between the central jet and the annular jet rapidly disappears. The structures of the LN_2 or LOX jets are bent backward, and it is assumed that the influence of the coaxial atomizer gas to atomization and mixing is much less effective, as previouly expected. In view of mixing, turbulence may play a more relevant role.

In the hot-fire case, during ignition and combustion the interface between the propellants is always separated and affected by a layer of hot reacting gas. The flame is attached to the LOX post. A diffusion flame resides within the annular post wake and is anchored by the small intensive recirculation zones that exist behind these posts. Radiation intensity of the flame strongly depends on chamber pressure and increases downstream. The spectrum of the flame ranges continuously from UV to IR. The dependency of line intensities on mixture ratio O/F was small, indicating that the combustion gases were undergoing various degrees of reaction with a wide distribution in gas temperature and composition.

Acknowledgments

Hot-fire tests have been done in cooperation with the National Aerospace Laboratory. The cooperation and the support of H. Tamura is gratefully acknowledged. The authors would like to thank G. Schneider for the realization of the cold-flow experiments and M. Oschwald for the evaluation of spectral data.

References

[1]Woodward, R., and Talley, D., "Raman Imaging of Transcritical Cryogenic Propellants," AIAA 96-0468, Jan. 1996.

[2]Mayer, W., "Coaxial Atomization of a Round Liquid Jet in a High Speed Gas Stream: A Phenomenological Study," *Experiments in Fluids*, Vol. 16, No. 6, 1994, pp. 401–410.

[3]Mayer, W., and Tamura, H., "Flow Visualization of Supercritical Propellant Injection in a Firing LOX/GH2 Rocket Engine," *Journal of Propulsion and Power*, Vol. 12, No.6, 1996, pp. 1137–1147.

[4]Mayer, W., Schik, A., Vieille, B., Chaveau, C., Goekalp, I., Talley, D., and Woodward, R., "Atomization and Breakup of Cryogenic Propellants Under High-Pressure Subcritical and Supercritical Conditions," *Journal of Propulsion and Power*, Vol. 14, No. 5, 1998, pp. 835–842.

[5]Mayer, W., and Krülle, G., "Rocket Engine Coaxial Injector Liquid/Gas Interface Flow Phenomena," *Journal of Propulsion and Power*, Vol. 11, No. 3, 1995, pp. 513–518.

[6]Gaydon, A. G., *The Spectroscopy of flames*, Chapman and Hall, London, Jan. 1974.

[7]Foust, M. J., Deshpande, M., Pal, S., Ni, T., Merkle, C. L., and Santoro, R. J., "Experimental and Analytical Characterization of a Shear Coaxial GO_2/GH_2 Flowfield," AIAA Paper 96-0646, 1996.

[8]Char, J. M., Kuo, K. K., and Hsieh, K. C., "Observations of Break-Up Processes of Liquid Jets Using Real-Time X-Ray Radiography," *Journal of Propulsion and Power*, Vol. 6, No. 5, 1990, pp. 544–551.